

# Isotopic evolution of the protoplanetary disk and the building blocks of Earth and the Moon

Martin Schiller<sup>1</sup>, Martin Bizzarro<sup>1</sup> & Vera Assis Fernandes<sup>2,3</sup>

Nucleosynthetic isotope variability among Solar System objects is often used to probe the genetic relationship between meteorite groups and the rocky planets (Mercury, Venus, Earth and Mars), which, in turn, may provide insights into the building blocks of the Earth–Moon system<sup>1–5</sup>. Using this approach, it has been inferred that no primitive meteorite matches the terrestrial composition and the protoplanetary disk material from which Earth and the Moon accreted is therefore largely unconstrained<sup>6</sup>. This conclusion, however, is based on the assumption that the observed nucleosynthetic variability of inner-Solar-System objects predominantly reflects spatial heterogeneity. Here we use the isotopic composition of the refractory element calcium to show that the nucleosynthetic variability in the inner Solar System primarily reflects a rapid change in the mass-independent calcium isotope composition of protoplanetary disk solids associated with early mass accretion to the proto-Sun. We measure the mass-independent <sup>48</sup>Ca/<sup>44</sup>Ca ratios of samples originating from the parent bodies of ureilite and angrite meteorites, as well as from Vesta, Mars and Earth, and find that they are positively correlated with the masses of their parent asteroids and planets, which are a proxy of their accretion timescales. This correlation implies a secular evolution of the bulk calcium isotope composition of the protoplanetary disk in the terrestrial planet-forming region. Individual chondrules from ordinary chondrites formed within one million years of the collapse of the proto-Sun<sup>7</sup> reveal the full range of inner-Solar-System mass-independent <sup>48</sup>Ca/<sup>44</sup>Ca ratios, indicating a rapid change in the composition of the material of the protoplanetary disk. We infer that this secular evolution reflects admixing of pristine outer-Solar-System material into the thermally processed inner protoplanetary disk associated with the accretion of mass to the proto-Sun. The identical calcium isotope composition of Earth and the Moon reported here is a prediction of our model if the Moon-forming impact involved protoplanets or precursors that completed their accretion near the end of the protoplanetary disk's lifetime.

A protoplanetary disk forms as a result of mass accretion from the collapse of the envelope onto the star. The rate of mass accretion onto the star via the disk is typically high in the early stages, resulting in elevated temperatures within a few astronomical units of the star<sup>8</sup>. In the Solar System, mass accretion to the proto-Sun resulted in thermal processing of pristine infalling molecular-cloud material, including the selective destruction of presolar carriers of nucleosynthetic isotope anomalies. This process is revealed by the correlated variability in the abundance of nuclides of distinct nucleosynthetic origin, such as <sup>46</sup>Ti–<sup>50</sup>Ti and <sup>43</sup>Ca–<sup>46</sup>Ca–<sup>48</sup>Ca, among Solar System reservoirs<sup>2,3</sup>. Parent bodies of meteorites formed from inner, thermally processed disk material show depletions in these isotopes relative to bodies formed in the outer-disk regions. The mass-independent isotopic compositions of various elements can therefore characterize the source of the precursor material to the rocky planets. However, this requires an understanding of the secular evolution of

the nucleosynthetic composition of the disk material that accreted to growing planetary bodies. Unlike nucleosynthetic tracers (such as Ti and Cr, which are present in planets as trace elements) and siderophile elements (such as Mo and Ru, which can help identify the source of the metal fraction of a body), calcium is one of the main constituents of rock-forming minerals and hence provides robust constraints on the precursor material to the rocky planets. To probe the Ca isotope evolution of the protoplanetary disk, we determined the mass-independent <sup>48</sup>Ca composition of selected Solar System objects, including ordinary and carbonaceous chondrites, ureilites, eucrites, angrites, martian and lunar meteorites, as well as individual chondrules from ordinary and carbonaceous chondrites (Fig. 1). We report the mass-independent Ca data as  $\mu^{48}\text{Ca}$  values, which express the calcium isotope composition of the sample relative to that of the SRM 915b standard:  $\mu^{48}\text{Ca} = [(^{48}\text{Ca}/^{44}\text{Ca})_{\text{sample}} / (^{48}\text{Ca}/^{44}\text{Ca})_{\text{SRM915b}} - 1] \times 10^6$ .

The growth of asteroids and Mars-sized embryos can result from the gas-drag-assisted accretion of millimetre-sized chondrules within about

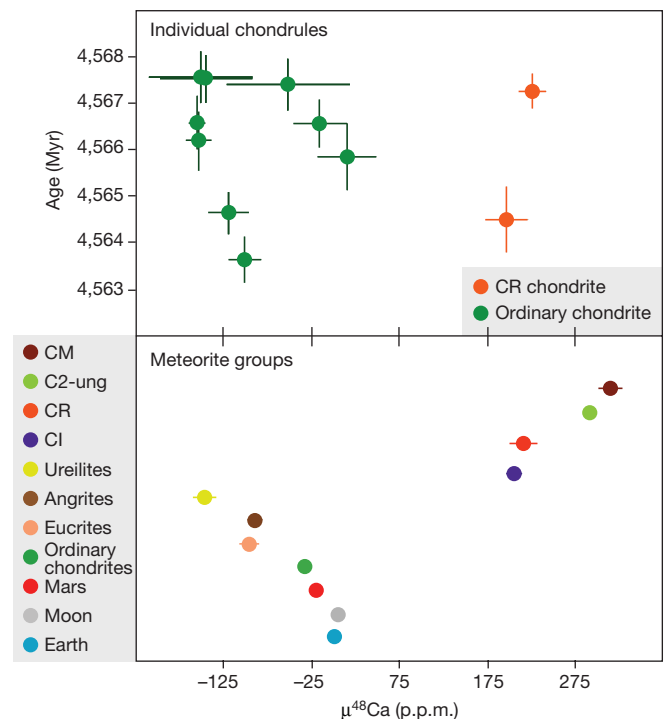


**Figure 1 | Mass-independent  $\mu^{48}\text{Ca}$  data for individual chondrules and bulk meteorites.** Chondrule data are shown versus their age<sup>7</sup>, as determined by Pb–Pb dating. Bulk rock  $\mu^{48}\text{Ca}$  data are shown as a Caltech plot. Uncertainties are two standard deviations for Pb–Pb ages and two standard errors of the mean for  $\mu^{48}\text{Ca}$  values. CM, Mighei-type chondrites; C2-ung, ungrouped carbonaceous chondrite of petrological type 2.

<sup>1</sup>Centre for Star and Planet Formation and Natural History Museum of Denmark, University of Copenhagen, Øster Voldgade 5–7, DK-1350, Denmark. <sup>2</sup>Museum für Naturkunde, Leibniz-Institut für Evolutions- und Biodiversitätsforschung, Berlin 10115, Germany. <sup>3</sup>Instituto Dom Luiz, Faculdade de Ciências, Universidade de Lisboa, 1749-016 Lisboa, Portugal.

3 million years (Myr)<sup>9,10</sup>. The ages obtained by U-corrected Pb–Pb dating and the initial Pb isotope compositions of the chondrules studied indicate a primary formation age restricted to the first million years of disk evolution, although some objects were remelted at later times<sup>7</sup>. Thus, these chondrules provide insights into the spatial and temporal evolution of the  $\mu^{48}\text{Ca}$  value of disk solids at early times (Fig. 1). The CR chondrite (Renazzo-type) chondrules have calcium isotope compositions comparable to those of CI carbonaceous (Ivuna-type) chondrites, indicating that their precursor material escaped extensive thermal processing. By contrast, ordinary chondrite chondrules show variable  $\mu^{48}\text{Ca}$  values, ranging from terrestrial values to  $\mu^{48}\text{Ca}$  deficits of  $-161 \pm 27$  p.p.m., where the uncertainties represent twice the standard error of the mean. Our bulk meteorite data are consistent with the conclusions of earlier studies<sup>3,11</sup>, namely, that bodies formed in the inner disk show systematic depletions in  $^{48}\text{Ca}$ , whereas carbonaceous outer-Solar-System bodies exhibit  $^{48}\text{Ca}$  excesses relative to Earth (Fig. 1).

Given the analytical uncertainty in the ages of individual chondrules, it is difficult to distinguish whether their  $^{48}\text{Ca}$  deficits relative to the solar composition reflect spatial heterogeneity or temporal evolution of the bulk composition of inner-disk solids. Astronomical observations of young stars and their disks indicate that the main accretion epoch of thermally unprocessed envelope material occurs over timescales comparable to those of primary chondrule formation, namely, during the first million years of disk evolution<sup>12</sup>. Assuming that CI chondrites have approximately the average composition of the envelope material, admixing this material into the inner disk will result in a progressive increase in the  $\mu^{48}\text{Ca}$  value of solids and bodies formed during this epoch. To test this hypothesis, we turn to the calcium isotope composition of differentiated asteroids and planetary bodies because their  $\mu^{48}\text{Ca}$  values reflect the average compositions of their precursors throughout the accretion history of these bodies.

Recent models<sup>9,10</sup> of the formation and growth of asteroidal bodies and planetary embryos suggest a two-stage process, where first-generation bodies with characteristic sizes of about 100 km form rapidly by streaming instabilities, followed by continuous growth dominated by gas-drag-assisted accretion of millimetre-sized particles for bodies with radii larger than about 200 km. This results in the formation of Mars-sized embryos over typical disk lifetimes of less than 5 Myr. Importantly, formation of the first embryos leads to the excitation of the inclinations of the smaller asteroids, which disconnects the asteroids from the chondrules in the mid-plane layer and hence terminates their accretion. Assuming a similar rate of accretion in the terrestrial-planet-forming region, these models predict that the final mass of a rocky body is a function of its accretion timescale. Although the masses of Earth, Mars and Vesta (the parent body of howardite, eucrite and diogenite meteorites<sup>13</sup>) can be inferred, the parent bodies of ureilite and angrite meteorites are not known. However, the presence of a core dynamo in the angrite parent body<sup>14</sup>, magmatic differentiation, and volcanic evolution indicate a similar thermal history to Vesta<sup>15,16</sup>, and the retention of basaltic lavas on its surface suggests that the angrite parent body may have been comparable in size to Vesta. The mass of the ureilite parent body was calculated using a density of  $3.22 \text{ g cm}^{-3}$  and a radius of  $105 \pm 25 \text{ km}$  (refs 17 and 18). We note that the absence of basaltic meteorites from the ureilite parent body, which could indicate loss of basaltic lavas through explosive volcanism, is consistent with a radius no larger than 100 km (ref. 19). Figure 2a shows that the  $^{48}\text{Ca}$  composition of differentiated bodies in the inner Solar System systematically increases with mass, indicating a secular evolution of the time-integrated average  $^{48}\text{Ca}$  composition of the disk material that accreted to form the terrestrial planets. Thus, the inner-disk  $^{48}\text{Ca}$  nucleosynthetic variations predominantly reflect progressive admixing of pristine matter from the outer Solar System into an initially thermally processed dust reservoir during the early stages of disk evolution. This establishes that the nucleosynthetic variability recorded by inner-disk bodies is primarily controlled by the formation timescales of their

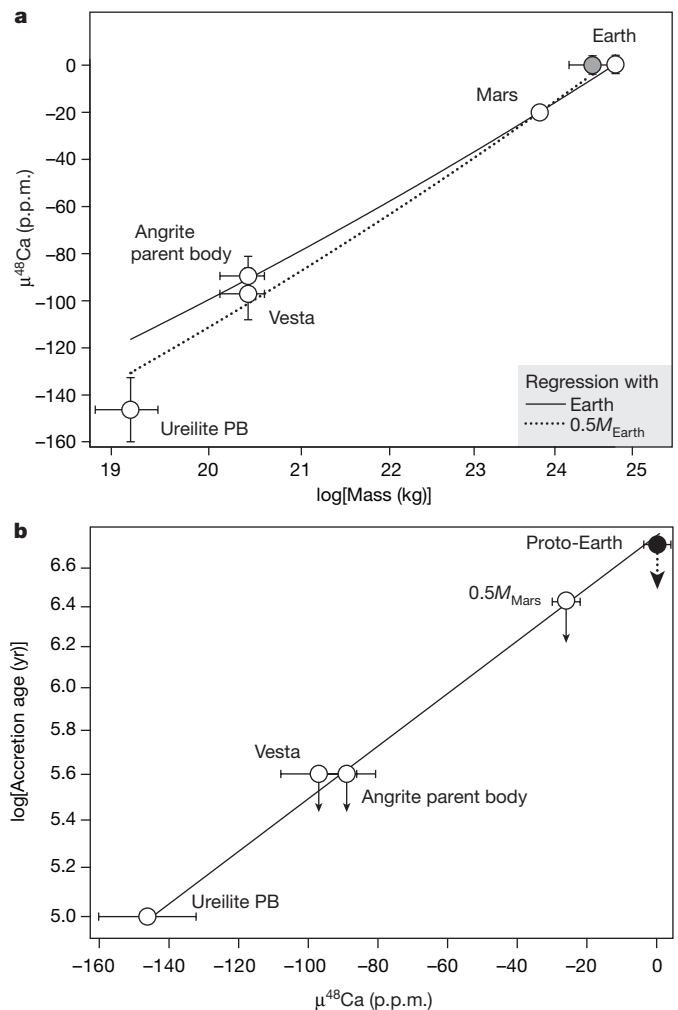


**Figure 2 | The  $\mu^{48}\text{Ca}$  value of planetary bodies versus their mass and their maximum accretion age.** **a**, Comparison between  $\mu^{48}\text{Ca}$  values of the ureilite parent body, the angrite parent body, Vesta, Mars and Earth with their respective masses on a logarithmic scale. The solid line is a linear least-squares fit ( $y = a + b \times x$ ), where  $a = -517.08 \pm 0.11$  and  $b = 20.878 \pm 0.005$ , and the uncertainties correspond to one standard deviation. We assigned 50% uncertainty to the masses of the angrite parent body and the eucrite parent body (Vesta). The dotted line shows a regression through the data assuming a precursor with mass  $(0.50 \pm 0.25)M_{\text{Earth}}$ , where  $M_{\text{Earth}}$  is Earth's mass. Regressions to data obtained using alternative masses for the ureilite parent body and Earth (precursors) are shown in Extended Data Fig. 1. **b**, Accretion ages of the ureilite parent body, the angrite parent body, Vesta, the proto-Earth, and Mars at half of its current mass (see Methods and refs 20, 21 and 23), shown in a logarithmic scale with respect to the formation of the Solar System, versus the  $\mu^{48}\text{Ca}$  values of their parent bodies. Downward arrows indicate that the accretion ages shown are upper limits. A linear regression with  $a = 6.7232$  and  $b = 0.011886$  is used to calculate the accretion age of the proto-Earth at 5.3 Myr on the basis of its  $\mu^{48}\text{Ca}$  value. The accretion age of the proto-Earth probably reflects the accretion age of its precursors, which may include a number of planetary embryos. Thus, Earth's final accretion occurred after disk dissipation from colliding embryos. The formation of a 0.9-Earth-mass object at 1 AU from the Sun within 5 Myr is possible via pebble accretion<sup>10</sup>, although early accretion of the proto-Earth is inconsistent with the present-day W isotope composition of Earth's mantle<sup>33</sup>. However, a better understanding of the W isotope evolution of the proto-Earth in the framework of pebble accretion and a thorough assessment of the extent of metal–silicate fractionation during the Moon-forming impact are required to evaluate this model.

precursors. This interpretation is generally consistent with data from other nucleosynthetic tracers of lithophile affinity when considering the uncertainties of the data (see Methods).

The inner-Solar-System chondrules investigated here suggest that the  $\mu^{48}\text{Ca}$  value of disk solids evolved from an ureilite-like to a terrestrial composition within about 1 Myr of the formation of the Solar System. Although these data indicate a rapid isotopic evolution of accreting disk solids, they provide no constraints on the rate of change of the average bulk composition of the inner disk. However, this information can be obtained from the  $\mu^{48}\text{Ca}$  values of differentiated asteroids and planetary bodies because their composition reflects the time-integrated average of the disk composition at the time of their accretion. Two ordinary chondrite chondrules that have U-corrected Pb–Pb ages within about 100,000 years of the formation of the Solar System have  $\mu^{48}\text{Ca}$  values identical to that of the ureilite parent body—the differentiated asteroid with the largest  $\mu^{48}\text{Ca}$  deficit. Short-lived-radionuclide chronology and thermal modelling indicate that the ureilite parent body completed its accretion less than 100,000 years from the formation of the Solar System (see Methods). Collectively, these observations suggest that the ureilite  $\mu^{48}\text{Ca}$  value of  $-146 \pm 14$  p.p.m. represents an inner-disk dust reservoir initially depleted in  $^{48}\text{Ca}$  through thermal processing. When Vesta and the angrite parent bodies accreted, less than  $0.25 \pm 0.15$  Myr from the formation of the Solar System<sup>20,21</sup>, the time-integrated average  $\mu^{48}\text{Ca}$  of inner-disk rocky bodies had evolved to  $-93.2 \pm 7.1$  p.p.m., and it reached  $-20.0 \pm 2.8$  p.p.m. and  $0.2 \pm 3.9$  p.p.m., respectively, when Mars and the precursor(s) of Earth completed their accretion.

It has been established that the protoplanetary disk was dissipated at the time of the formation of the impact-generated CB (Bencubbin-type) Gujba chondrite chondrules,  $4,562.49 \pm 0.21$  million years ago<sup>22</sup>, implying cessation of the infall of outer-Solar-System material to the inner disk. Thus, the timing of disk dissipation marks a transition point, after which the  $\mu^{48}\text{Ca}$  value of inner-disk bodies can no longer be modified by infall. Given the observed relationship between  $\mu^{48}\text{Ca}$  values and planetary masses (Fig. 2a), the timing of the accretion of Earth's precursor can be deduced, assuming that the accretion timescales of Mars, Vesta, and the angrite and ureilite parent bodies are well understood. Hf–W systematics of martian meteorites<sup>23</sup> suggest that Mars reached half of its mass  $1.8^{+0.9}_{-1.0}$  Myr after the formation of the Solar System, whereas thermal modelling and  $^{26}\text{Al}$ – $^{26}\text{Mg}$  data constrain the accretion of Vesta and the angrite parent body to less than 0.4 Myr<sup>20,21</sup>. Accretion of the ureilite parent body is believed to have been completed by about 0.1 Myr after the formation of the Solar System to ensure partial differentiation from the decay of  $^{26}\text{Al}$  (see Methods). Using these estimates, we show in Fig. 2b that accretion of the proto-Earth or its precursors, which may include a number of planetary embryos (see Fig. 2 legend), was completed within about 5.3 Myr. These observations suggest that the  $\mu^{48}\text{Ca}$  value of Earth represents the average bulk inner-disk composition before its dissipation. The addition rate of material from the outer Solar System to the inner disk can be evaluated from the secular change in the average inner-disk  $^{48}\text{Ca}$  composition, which is inferred from differentiated asteroids and planets. Accepting an ureilite-like  $\mu^{48}\text{Ca}$  value for the bulk inner disk at 0.1 Myr, we show in Fig. 3a that the rate of addition of material from the outer Solar System to the inner disk mirrors the typical mass accretion rates of low-mass protostars<sup>24</sup>. Therefore, this flux of material appears to be associated with the infall of envelope material and hence the growth of the proto-Sun.

Our model for the secular  $\mu^{48}\text{Ca}$  evolution of the inner protoplanetary disk provides insights into the nature of the precursor material to planetesimals and planets. The compositions of Vesta and the angrite parent body require mixing of 15% of thermally unprocessed CI-like material with their precursors. For Mars and the proto-Earth, the amount of thermally unprocessed material needed to account for their bulk  $\mu^{48}\text{Ca}$  values is 36% and 42%, respectively. If correct, these evaluations imply that more than half of the mass of the inner disk was already locked into asteroidal bodies or planetary embryos about 100,000 years after the collapse of the proto-Sun (Fig. 3b). Thus, the  $\mu^{48}\text{Ca}$  values of terrestrial planets reflect their accretion histories throughout the lifetime of the disk. By contrast, most chondrites represent fragments of bodies formed during the late stages of accretion and, as such, can

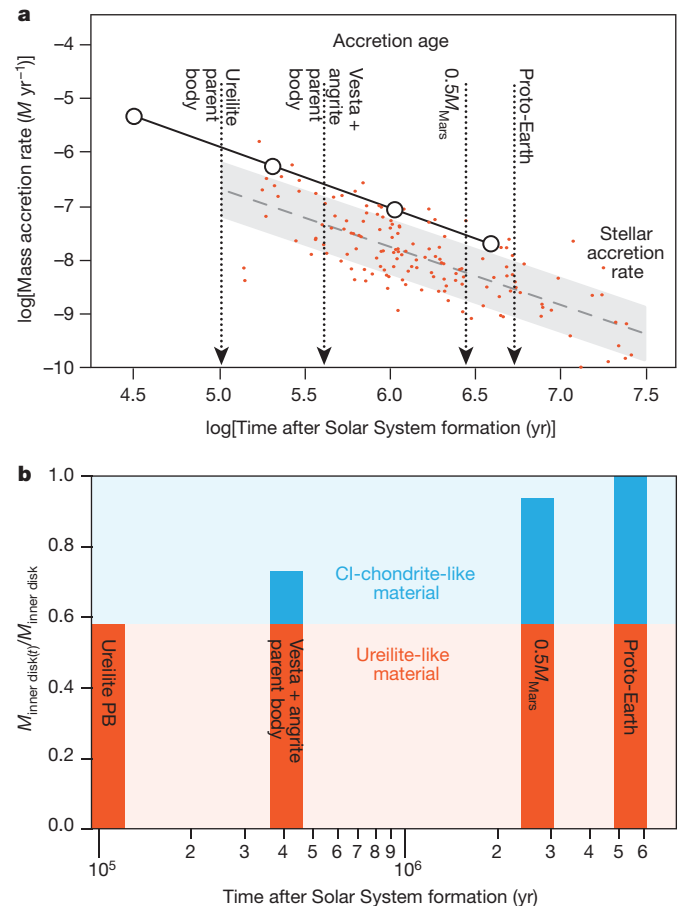


**Figure 3 | Accretion rate of inner-disk mass versus time.** **a**, Mass accretion rates (in inner-disk masses,  $M$ , per year) of the inner protoplanetary disk, calculated from the  $\mu^{48}\text{Ca}$  values and maximum accretion timescales of planetary bodies (white circles), assuming that the  $\mu^{48}\text{Ca}$  signature of a body is representative of the entire inner-disk mass at that time. Therefore, the accretion rate of the inner protoplanetary disk reflects the amount of mass locked inside bodies at any given time relative to the final disk mass, which is taken as the mass of asteroids, moons and planets located sunwards of Jupiter (see Methods). Given the apparent power-law decline in the accretion rates, we show each calculated value at the logarithmic centre of the corresponding time interval,  $\Delta\log(t)/2$ , where  $t$  is the time after the formation of the Solar System. For comparison, we also show observed stellar accretion rates (in solar masses,  $M_{\odot}$ , per year) for  $0.3M_{\odot}$ – $M_{\odot}$  objects (red dots) scaled to a  $0.7M_{\odot}$  star, as well as the best linear fit (dashed line) and one standard deviation (shaded area) of these data<sup>24</sup>. **b**, Proportion of mass locked inside asteroids, embryos and planets at their maximum accretion age ( $M_{\text{inner disk}}(t)/M_{\text{inner disk}}$ ), assuming that the composition of each parent body is representative of the bulk disk at the time of accretion. The fractions are calculated as mixtures between a ureilite-like  $\mu^{48}\text{Ca}$  value and outer-Solar-System dust, represented by CI chondrites (see Methods).

at best represent only a snapshot of the disk composition at the time of their accretion. However, given the small size of their parent bodies, it is unclear whether their compositions are representative of the average accreting material at the time of their formation, which can be also influenced by variable proportions of chondrule and matrix. For example, the ordinary chondrite chondrules analysed here have a weighted average  $\mu^{48}\text{Ca}$  of  $-129 \pm 50$  p.p.m., making the bulk rock composition very sensitive to the chondrule-to-matrix ratio. Thus, chondrites cannot be used to assess the nature of the precursor material to rocky planets reliably.

To explain the observed nucleosynthetic dichotomy between inner- and outer-Solar-System bodies, it has been proposed<sup>25</sup> that the transport of material from the outer Solar System to the inner disk

was stopped by the opening of a disk gap related to the formation of Jupiter's core, about 1 Myr after the formation of the Sun. However, numerical simulations and astronomical observations suggest that such an opening would not quench mass accretion to the protostar, but would limit the inward transport of large dust grains by filtration<sup>26,27</sup>. Coagulation of smaller dust particles Sunwards of the disk gap would continue to fuel planetary growth by pebble accretion. The apparent lack of this material in ordinary chondrites may reflect the fact that the main growth mechanism of small bodies—namely, the streaming instability—is less efficient in accreting smaller particles. Testing this hypothesis, however, requires numerical simulations that better describe the relationship between size sorting during planetesimal formation by the streaming instability and size sorting by pebble accretion. Lastly, our results and interpretations imply that more than half of the mass of the inner disk was already locked into sizeable bodies with a  $\mu^{48}\text{Ca}$  values similar to that of ureilites about 100,000 years after the collapse of the proto-Sun (Fig. 3b). Taking into account mass balance, mixing of pristine CI-like dust from the outer Solar System with this inner-disk reservoir can at most raise the bulk  $\mu^{48}\text{Ca}$  value of the disk to approximately the terrestrial one, thereby preserving an isotopic contrast between rocky planets and carbonaceous asteroidal bodies. Therefore, we infer that the nucleosynthetic dichotomy between inner- and outer-Solar-System bodies reflects the rapid accretion of thermally processed disk material into asteroidal bodies or planetary embryos and does not require the early formation of a disk gap.

The giant impact theory for the formation of the Earth–Moon system proposes that a Mars-sized embryo collided with the proto-Earth and ejected material into an Earth-orbiting disk, which subsequently accumulated into the Moon<sup>28</sup>. Because models predict that most of the Moon's mass is derived from the impactor, this theory is difficult to reconcile with the nearly identical isotopic compositions of Earth and the Moon for lithophile elements<sup>1,5,29</sup>. Therefore, a number of alternative models have been proposed that allow for disk–planet compositional equilibration<sup>30–32</sup>. Our high-precision data define a  $\mu^{48}\text{Ca}$  value of  $3.7 \pm 1.9$  p.p.m. for the Moon. In the framework of the canonical model<sup>29</sup>, this requires the  $\mu^{48}\text{Ca}$  values of the proto-Earth and the impactor to be within 10 p.p.m. of each other. Our results suggest that the bulk  $\mu^{48}\text{Ca}$  composition of the inner protoplanetary disk evolved to a terrestrial composition within about 5 Myr (Fig. 2b), so the isotopic similarity between Earth and the Moon can be explained if the giant impact involved bodies or precursors that completed their accretions towards the end of the disk's lifetime. The nearly identical isotope signatures of Earth and the Moon are thus an outcome of the evolving isotopic composition of the disk.

**Online Content** Methods, along with any additional Extended Data display items and Source Data, are available in the online version of the paper; references unique to these sections appear only in the online paper.

**Received 28 July 2017; accepted 22 January 2018.**

- Zhang, J., Dauphas, N., Davis, A. M., Leya, I. & Fedkin, A. The proto-Earth as a significant source of lunar material. *Nat. Geosci.* **5**, 251–255 (2012).
- Trinquier, A. *et al.* Origin of nucleosynthetic isotope heterogeneity in the solar protoplanetary disk. *Science* **324**, 374–376 (2009).
- Schiller, M., Paton, C. & Bizzarro, M. Evidence for nucleosynthetic enrichment of the protosolar molecular cloud core by multiple supernova events. *Geochim. Cosmochim. Acta* **149**, 88–102 (2015).
- Dauphas, N. The isotopic nature of the Earth's accreting material through time. *Nature* **541**, 521–524 (2017).
- Young, E. D. *et al.* Oxygen isotopic evidence for vigorous mixing during the Moon-forming giant impact. *Science* **351**, 493–496 (2016).
- Burkhardt, C. *et al.* In search of the Earth-forming reservoir: mineralogical, chemical, and isotopic characterizations of the ungrouped achondrite NWA 5363/NWA 5400 and selected chondrites. *Meteorit. Planet. Sci.* **52**, 807–826 (2017).
- Bollard, J. *et al.* Early formation of planetary building blocks inferred from Pb isotopic ages of chondrules. *Sci. Adv.* **3**, e1700407 (2017).
- Ciesla, F. J. Radial transport in the solar nebula: implications for moderately volatile element depletions in chondritic meteorites. *Meteorit. Planet. Sci.* **43**, 639–655 (2008).

- Lambrechts, M. & Johansen, A. Rapid growth of gas-giant cores by pebble accretion. *Astron. Astrophys.* **544**, A32 (2012).
- Johansen, A., Mac Low, M. M., Lacerda, P. & Bizzarro, M. Growth of asteroids, planetary embryos, and Kuiper belt objects by chondrule accretion. *Sci. Adv.* **1**, e1500109 (2015).
- Dauphas, N. *et al.* Calcium-48 isotopic anomalies in bulk chondrites and achondrites: evidence for a uniform isotopic reservoir in the inner protoplanetary disk. *Earth Planet. Sci. Lett.* **407**, 96–108 (2014).
- Currie, T. & Sicilia-Aguilar, A. The transitional protoplanetary disk frequency as a function of age: disk evolution in the Coronet Cluster, Taurus, and other 1–8 Myr old regions. *Astrophys. J.* **732**, 24 (2011).
- McSween, H. Y. *et al.* Dawn; and the Vesta–HED connection; and the geologic context for eucrites, diogenites, and howardites. *Meteorit. Planet. Sci.* **48**, 2090–2104 (2013).
- Wang, H. *et al.* Lifetime of the solar nebula constrained by meteorite paleomagnetism. *Science* **355**, 623–627 (2017).
- Schiller, M., Baker, J. A. & Bizzarro, M. <sup>26</sup>Al–<sup>26</sup>Mg dating of asteroidal magmatism in the young Solar System. *Geochim. Cosmochim. Acta* **74**, 4844–4864 (2010).
- Keil, K. Angrites, a small but diverse suite of ancient, silica-undersaturated volcanic-plutonic mafic meteorites, and the history of their parent asteroid. *Chem. Erde* **72**, 191–218 (2012).
- Macke, R. J., Britt, D. T. & Consolmagno, G. J. Density, porosity, and magnetic susceptibility of achondritic meteorites. *Meteorit. Planet. Sci.* **46**, 311–326 (2011).
- Wilson, L., Goodrich, C. A. & Van Orman, J. A. Thermal evolution and physics of melt extraction on the ureilite parent body. *Geochim. Cosmochim. Acta* **72**, 6154–6176 (2008).
- Wilson, L. & Keil, K. Volcanic activity on differentiated asteroids: a review and analysis. *Chem. Erde* **72**, 289–321 (2012).
- Schiller, M. *et al.* Rapid timescales for magma ocean crystallization on the howardite–eucrite–diogenite parent body. *Astrophys. J. Lett.* **740**, L22 (2011).
- Schiller, M., Connelly, J. N., Glad, A. C., Mikouchi, T. & Bizzarro, M. Early accretion of protoplanets inferred from a reduced inner solar system <sup>26</sup>Al inventory. *Earth Planet. Sci. Lett.* **420**, 45–54 (2015).
- Bollard, J., Connelly, J. N. & Bizzarro, M. Pb–Pb dating of individual chondrules from the CBa chondrite Gujba: assessment of the impact plume formation model. *Meteorit. Planet. Sci.* **50**, 1197–1216 (2015).
- Dauphas, N. & Pourmand, A. Hf–W–Th evidence for rapid growth of Mars and its status as a planetary embryo. *Nature* **473**, 489–492 (2011).
- Hartmann, L., Herczeg, G. & Calvet, N. Accretion onto pre-main-sequence stars. *Annu. Rev. Astron. Astrophys.* **54**, 135–180 (2016).
- Kruijer, T. S., Burkhardt, C., Budde, G. & Kleine, T. Age of Jupiter inferred from the distinct genetics and formation times of meteorites. *Proc. Natl Acad. Sci. USA* **114**, 6712–6716 (2017).
- Picogna, G. & Kley, W. How do giant planetary cores shape the dust disk? HL Tauri system. *Astron. Astrophys.* **584**, A110 (2015).
- Carrasco-González, C. *et al.* The VLA view of the HL Tau disk: disk mass, grain evolution, and early planet formation. *Astrophys. J. Lett.* **821**, L16 (2016).
- Hartmann, W. K. & Davis, D. R. Satellite-sized planetesimals and lunar origin. *Icarus* **24**, 504–515 (1975).
- Canup, R. M. Lunar-forming impacts: processes and alternatives. *Phil. Trans. R. Soc. A* **372**, 20130175 (2014).
- Canup, R. M. Forming a Moon with an Earth-like composition via a giant impact. *Science* **338**, 1052–1055 (2012).
- Čuk, M. & Stewart, S. T. Making the Moon from a fast-spinning Earth: a giant impact followed by resonant despinning. *Science* **338**, 1047–1052 (2012).
- Meier, M. M. M., Reufer, A. & Wieler, R. On the origin and composition of Theia: constraints from new models of the Giant Impact. *Icarus* **242**, 316–328 (2014).
- Kleine, T. *et al.* Hf–W chronology of the accretion and early evolution of asteroids and terrestrial planets. *Geochim. Cosmochim. Acta* **73**, 5150–5188 (2009).

**Acknowledgements** Financial support for this project was provided to M.B. by the Danish National Research Foundation (DNRF97) and the European Research Council (ERC Consolidator Grant Agreement 616027—STARJUSTASTEROIDS). V.A.F. acknowledges financial support from a DFG-Eigenstelle FE 1523/3-1 and the Royal Society for the purchase of Dhofer 287. We thank Å. Nordlund, A. Johansen and F. Moynier for discussion on the paper, as well as J. Day for comments that helped improve the quality of our paper.

**Author Contributions** M.S. and M.B. designed the study and experiments. M.S. conducted the analytical work. All authors participated in the interpretation of the data. M.S. and M.B. wrote the manuscript with input from V.A.F.

**Author Information** Reprints and permissions information is available at [www.nature.com/reprints](http://www.nature.com/reprints). The authors declare no competing financial interests. Readers are welcome to comment on the online version of the paper. Publisher's note: Springer Nature remains neutral with regard to jurisdictional claims in published maps and institutional affiliations. Correspondence and requests for materials should be addressed to M.S. ([schiller@snm.ku.dk](mailto:schiller@snm.ku.dk)).

**Reviewer Information** *Nature* thanks J. Day and the other anonymous reviewer(s) for their contribution to the peer review of this work.

## METHODS

**Sample preparation and isotope analyses.** Bulk samples weighing 20–100 mg were digested in a HF-HNO<sub>3</sub> medium in Parr bombs at 210 °C for 2–3 days. Calcium was also separated from sample digestions of nine chondrules extracted from the ordinary chondrite (L3.10) NWA 5697 and two chondrules from the CR2 sample NWA 6043, which have previously been analysed for Pb isotopes<sup>7</sup>. The individual sample dissolutions typically represent less than 10 mg of sampled chondrule material, which is significantly smaller than the amount of processed bulk meteorite samples. Following complete dissolution of the samples, Ca was separated from the sample matrix by ion-exchange chromatography<sup>34</sup> in a four-step procedure. Although this technique is usually efficient, all samples were monitored for the presence of contaminant elements, such as Mg, Sr and Ti, in the purified-Ca solution. Individual chromatography separation steps were repeated when the presence of contaminants could affect the analysis (for example, when the Sr/Ca concentration ratio was higher than  $1 \times 10^{-6}$ ). The isotopic compositions of the purified-Ca separates were measured with a Neptune Plus multiple-collector inductively coupled plasma mass spectrometer (MC-ICPMS) at the Centre for Star and Planet Formation (Natural History Museum of Denmark, University of Copenhagen) by following established analytical procedures<sup>3,34</sup>. Data were acquired in the static mode using six Faraday collectors, one for each of the isotopes <sup>48</sup>Ca, <sup>47</sup>Ti, <sup>46</sup>Ca, <sup>42</sup>Ca, <sup>43</sup>Ca and <sup>44</sup>Ca. The Faraday cup used for <sup>47</sup>Ti was connected to an amplifier with a  $10^{12} \Omega$  feedback resistor, whereas the other collectors were connected to amplifiers with  $10^{11} \Omega$  feedback resistors. Samples were aspirated into the plasma source by means of an Apex sample introduction system with an uptake rate of  $20 \mu\text{l min}^{-1}$ , and the Ca isotopes were measured with a mass resolving power ( $M/\Delta M$ , as defined by the peak edge width from 5% to 95% at full peak height) that was always greater than 5,000. The sensitivity under these analytical conditions was approximately  $300 \text{ V (p.p.m.)}^{-1}$ .

Given the low abundance of the <sup>46</sup>Ca nuclide and the limited <sup>43</sup>Ca variability (lower than 20 p.p.m.) between bulk inner-Solar-System reservoirs relative to the measurement uncertainty (about 2 p.p.m.)<sup>3,34</sup>, we focus on the high-precision determination of the mass-independent <sup>48</sup>Ca/<sup>44</sup>Ca ratio,  $\mu^{48}\text{Ca}$ , which we measure with an external reproducibility of 12 p.p.m. for individual sample analyses<sup>34</sup>. We also report the mass-dependent <sup>42</sup>Ca/<sup>44</sup>Ca ( $\delta^{42/44}\text{Ca}$ ) and <sup>43</sup>Ca/<sup>44</sup>Ca ( $\delta^{43/44}\text{Ca}$ ) values with respect to SRM 915b, which are calculated in the same way as  $\mu^{48}\text{Ca}$ , but are not corrected for mass fractionation. For each sample of sufficient size, the analysis consists of 15–20 sample measurements, each of which comprises 839 s of data acquisition and 340 s of baseline measurements and is bracketed by measurements of the SRM 915b standard. For individual chondrules, both the signal intensity and the number of repeat analyses were adjusted to achieve the best possible precision, given the limited amount of Ca available in these samples. The data reduction was conducted off-line and changes in mass bias with time were interpolated using a smoothed cubic spline. For each analysis, the mean and standard error of the measured ratios were calculated using a three-standard-deviation threshold to reject outliers. Individual analyses of a sample were combined to produce an average weighted by the propagated uncertainties of individual analyses. The final uncertainties reported here are twice the standard error of the mean.

**Calculation of disk-mass accretion rates.** For simplicity, we assume that the mass of asteroids, moons and planets located sunwards of Jupiter represents the final mass of the protoplanetary disk and the  $\mu^{48}\text{Ca}$  signature of Earth, which makes up 50% of this mass, is representative of the final inner-disk composition. This assumption is justified because  $\mu^{48}\text{Ca}$  reveals the composition of disk solids, but not that of gas. The mass accreted in bodies at any given time is assumed to be traced by the bulk  $\mu^{48}\text{Ca}$  signature of planetary bodies: increase in the  $\mu^{48}\text{Ca}$  value of planetary bodies represents an addition of material from the outer Solar System to the growing inner disk. In this simple two-component mixing model, the ureilite parent body represents the mean composition of the inner disk 0.1 Myr after the formation of the Solar System. The  $\mu^{48}\text{Ca}$  signature of CI chondrites represents the added outer-Solar-System material during the lifetime of the disk, and the  $\mu^{48}\text{Ca}$  signature of Earth corresponds to the final composition of the disk after accretion has ceased. This mixing model requires that 58.4% of the material had accreted by the time the ureilite parent body formed (less than 0.1 Myr after the formation of the Solar System). The subsequent increase in the bulk  $\mu^{48}\text{Ca}$  signatures of Vesta and the angrite parent body, Mars at half of its current mass and the proto-Earth represent addition of 15.0%, 19.6% and 6.9% outer-Solar-System material during the time intervals between the accretion of: 1) the ureilite parent body and Vesta (0.1–0.4 Myr), 2) Vesta and Mars at 50% of its present mass (0.4–2.7 Myr) and 3) Mars at 50% of its present mass and the proto-Earth (2.7–5.3 Myr), respectively. The amount of early-accreted material only increases if we assume the <sup>48</sup>Ca signature of carbonaceous chondrites other than CI chondrites. The change in accreted mass per time interval relative to the final disk mass (that is, 0.584, 0.150, 0.196

and 0.069 of the final inner-disk mass) allows us to calculate mean inner-disk mass accretion rates for each of the four intervals by dividing the added mass per time interval by its duration (0.1 Myr, 0.3 Myr, 2.3 Myr and 2.6 Myr, respectively). The resulting accretion rates are  $5.8 \times 10^{-6} M_{\text{inner disk}} \text{ yr}^{-1}$ ,  $5.0 \times 10^{-7} M_{\text{inner disk}} \text{ yr}^{-1}$ ,  $8.5 \times 10^{-8} M_{\text{inner disk}} \text{ yr}^{-1}$  and  $2.6 \times 10^{-8} M_{\text{inner disk}} \text{ yr}^{-1}$ , respectively.

**Timing of accretion of the ureilite parent body.** The energy release from the decay of the short-lived <sup>26</sup>Al radionuclide (half-life,  $t_{1/2} = 0.73 \text{ Myr}$ ) is the most important heat source driving differentiation on small planetary bodies that were accreted during the first few millions of years from the formation of the Solar System. Therefore, the timing of accretion of differentiated bodies can be determined by estimating the time needed for the parent body to achieve global melting from the energy released by <sup>26</sup>Al. This requires knowledge of the timing of differentiation, as well as the initial abundance of <sup>26</sup>Al in the body's precursor material. Recent studies have shown that canonical levels of <sup>26</sup>Al found in calcium–aluminium–rich inclusions (CAIs) are not representative of the majority of the matter that made up the terrestrial-planet-forming region<sup>21,35</sup>. Instead, the <sup>26</sup>Al/<sup>27</sup>Al abundance ratio in this region at the time of CAI formation probably had values between 1 and  $1.6 \times 10^{-5}$  (refs 21, 35). On the basis of <sup>26</sup>Al–<sup>26</sup>Mg and <sup>53</sup>Mn–<sup>53</sup>Cr systematics, initial magmatic differentiation of the ureilite parent body took place at  $4,567.1 \pm 1.1 \text{ Myr ago}$ <sup>36,37</sup>, which is the same age as the age of our Solar System based on CAI data<sup>38</sup>. Assuming that the initial <sup>26</sup>Al/<sup>27</sup>Al abundance in the material from which the ureilite parent body formed was  $1.3 \times 10^{-5}$  and the precursor material was ordinary chondrite-like in terms of density and composition, thermal modelling requires that the accretion was completed by 0.1 Myr after CAI formation. This is constrained by assuming an ambient temperature of 550 K in the accretion region of the ureilite parent body at about 0.1 Myr (ref. 39) and requires the parent body to achieve an internal temperature of 1,553 K, equivalent to 30% partial melting<sup>18</sup>, within 1.1 Myr after CAI formation, which is the time allowed by the age uncertainty for magmatic differentiation<sup>36,37</sup>. We note that this accretion age is consistent with independent estimates of the accretion time of the ureilite parent body<sup>40</sup>.

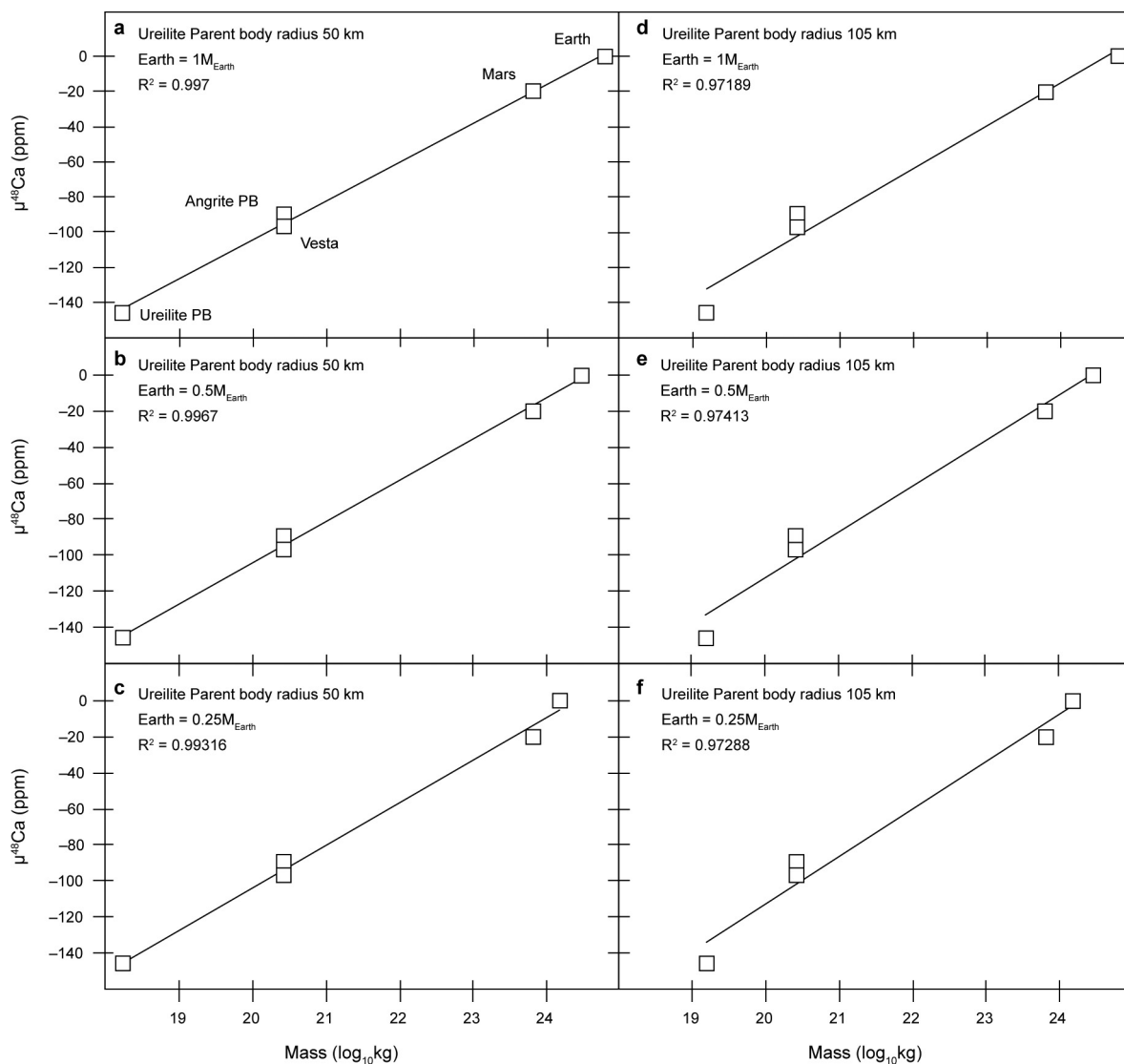
**Stable Ca isotope composition of meteorites and chondrules.** We also report the  $\delta^{42/44}\text{Ca}$  and  $\delta^{43/44}\text{Ca}$  values for our samples in Extended Data Table 1 and Extended Data Fig. 2 because mass-dependent fractionation can affect the accuracy of mass-independent  $\mu^{48}\text{Ca}$  data via inappropriate corrections for natural mass fractionation. For example, correcting the natural mass-dependent fractionation by using a kinetic law to retrieve the  $\mu^{48}\text{Ca}$  data will introduce an excess or deficit in  $\mu^{48}\text{Ca}$  if the natural fractionation is driven by non-kinetic processes<sup>34</sup>. Deviation from kinetic mass-dependent fractionation can occur during calcite precipitation<sup>41</sup> and during chemical weathering in arid environments<sup>42</sup>—the latter is relevant here because a number of our samples are hot-desert finds. Such corrections can change  $\mu^{48}\text{Ca}$  by up to 12 p.p.m. for a 0.1‰ difference in the  $\delta^{42/44}\text{Ca}$  value. The  $\delta^{42/44}\text{Ca}$  values that we report here are in excellent agreement with literature data for the same group of meteorites (Extended Data Fig. 3)<sup>43–45</sup>, confirming that the potential effects from such inadequate corrections are well within the uncertainty of our  $\mu^{48}\text{Ca}$  results. Our  $\delta^{42/44}\text{Ca}$  data for individual chondrules from ordinary and CR chondrites are also comparable to the value reported for CV chondrites in ref. 44. Moreover, we find no systematic differences (within uncertainty) in  $\mu^{48}\text{Ca}$  between hot-desert and non-hot-desert meteorites, or between falls versus finds, in the same differentiated group (that is, ureilites, angrites and Mars) (Extended Data Fig. 4). Potential effects from the addition of terrestrial Ca into lunar and martian meteorites can also be ruled out on the basis of mass balance considerations. For example, assuming that the pristine martian  $\mu^{48}\text{Ca}$  value is  $-20 \pm 2.8 \text{ p.p.m.}$  relative to that of Earth, the addition of 15% of terrestrial Ca, which would be clearly identifiable from hand specimens, would result in a change of only 3 p.p.m. This effect is well within the external reproducibility of our measurements. Given that the <sup>48</sup>Ca composition of the Moon is even closer to that of Earth's, addition of 15% terrestrial Ca to a lunar meteorite would result in even smaller effects than those of martian meteorites. These data demonstrate that stable or mass-independent Ca isotope data are not affected by terrestrial processes before meteorite recovery, within the uncertainty of our measurements.

**Other nucleosynthetic isotope data interpreted with our model.** Nucleosynthetic anomalies have been reported for a number of elements besides Ca, such as Ti, Cr, Ni, Sr, Nd, Mo, Ru and O<sup>1,2,6,46–59</sup>. Here we evaluate the consistency of our model with the isotope variability of these elements in various Solar System reservoirs. In this assessment, we consider whether it is possible to generate this nucleosynthetic variability in inner-Solar-System bodies by mixing a CI-like composition with a depleted inner-Solar-System dust with the composition of ureilite (where available) or angrite meteorites (Extended Data Fig. 5). On the basis of previous data<sup>1,2,6,46–54</sup>, our model is compatible with the variability of isotopes of lithophile elements, such as <sup>50</sup>Ti, <sup>54</sup>Cr, <sup>62</sup>Ni and <sup>145</sup>Nd, within the uncertainties of the data (Extended Data Fig. 5). Nucleosynthetic anomalous isotopes (isotopes with nucleosynthetic

signatures that differ from Earth's) of other elements either do not show significant variability beyond typical analytical uncertainties (such as  $^{84}\text{Sr}$ )<sup>55–57</sup>, or do not track the entire accretion history of planetary bodies (siderophile elements, such as Mo and Ru)<sup>4</sup>, or may be affected by other processes, such as gas–water interactions (for example, O). Therefore, we conclude that our model is consistent with the nucleosynthetic variability of elements that track the source of the silicate fraction of asteroidal and planetary bodies.

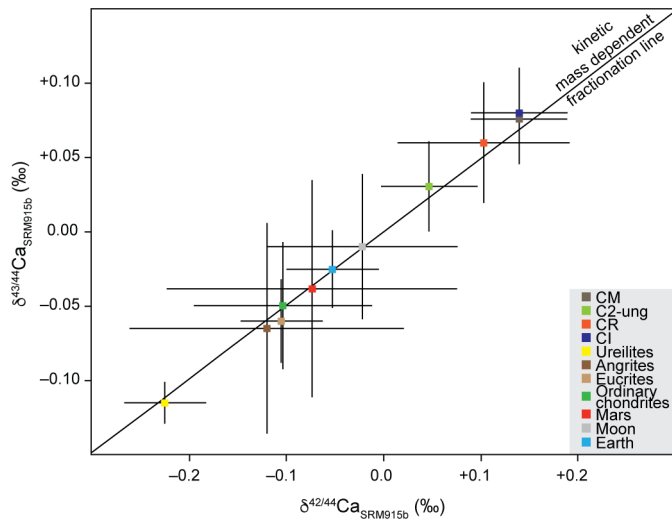
**Data availability.** Data supporting the findings of this study are available within the paper (including Methods and Extended Data) and from the EarthChem library (<http://dx.doi.org/10.1594/IEDA/100744>).

34. Schiller, M., Paton, C. & Bizzarro, M. Calcium isotope measurement by combined HR-MC-ICPMS and TIMS. *J. Anal. At. Spectrom.* **27**, 38–49 (2012).
35. Larsen, K. K. *et al.* Evidence for magnesium isotope heterogeneity in the solar protoplanetary disk. *Astrophys. J. Lett.* **735**, L37 (2011).
36. van Kooten, E. M., Schiller, M. & Bizzarro, M. Magnesium and chromium isotope evidence for initial melting by radioactive decay of  $^{26}\text{Al}$  and late stage impact-melting of the ureilite parent body. *Geochim. Cosmochim. Acta* **208**, 1–23 (2017).
37. Baker, J. A., Schiller, M. & Bizzarro, M.  $^{26}\text{Al}$ – $^{26}\text{Mg}$  deficit dating ultramafic meteorites and silicate planetesimal differentiation in the early Solar System? *Geochim. Cosmochim. Acta* **77**, 415–431 (2012).
38. Connelly, J. N. *et al.* The absolute chronology and thermal processing of solids in the solar protoplanetary disk. *Science* **338**, 651–655 (2012).
39. Estrada, P. R., Cuzzi, J. N. & Morgan, D. A. Global modeling of nebulae with particle growth, drift, and evaporation fronts. I. Methodology and typical results. *Astrophys. J.* **818**, 200 (2016).
40. Sugiura, N. & Fujiya, W. Correlated accretion ages and  $\epsilon^{54}\text{Cr}$  of meteorite parent bodies and the evolution of the solar nebula. *Meteorit. Planet. Sci.* **49**, 772–787 (2014).
41. Gussone, N. *et al.* Calcium isotope fractionation in calcite and aragonite. *Geochim. Cosmochim. Acta* **69**, 4485–4494 (2005).
42. Ewing, S. A. *et al.* Non-biological fractionation of stable Ca isotopes in soils of the Atacama Desert, Chile. *Geochim. Cosmochim. Acta* **72**, 1096–1110 (2008).
43. Valdes, M. C., Moreira, M., Foriel, J. & Moynier, F. The nature of Earth's building blocks as revealed by calcium isotopes. *Earth Planet. Sci. Lett.* **394**, 135–145 (2014).
44. Amsellem, E. *et al.* Testing the chondrule-rich accretion model for planetary embryos using calcium isotopes. *Earth Planet. Sci. Lett.* **469**, 75–83 (2017); corrigendum 474 527 (2017).
45. Magna, T., Gussone, N. & Mezger, K. The calcium isotope systematics of Mars. *Earth Planet. Sci. Lett.* **430**, 86–94 (2015).
46. Tang, H. & Dauphas, N. Abundance, distribution, and origin of  $^{60}\text{Fe}$  in the solar protoplanetary disk. *Earth Planet. Sci. Lett.* **359–360**, 248–263 (2012).
47. Tang, H. & Dauphas, N.  $^{60}\text{Fe}$ – $^{60}\text{Ni}$  chronology of core formation in Mars. *Earth Planet. Sci. Lett.* **390**, 264–274 (2014).
48. Zhang, J., Dauphas, N., Davis, A. M. & Pourmand, A. A new method for MC-ICPMS measurement of titanium isotopic composition: identification of correlated isotope anomalies in meteorites. *J. Anal. At. Spectrom.* **26**, 2197–2205 (2011).
49. Trinquier, A., Birck, J. L. & Allegre, C. J. Widespread  $^{54}\text{Cr}$  heterogeneity in the inner solar system. *Astrophys. J.* **655**, 1179–1185 (2007).
50. Yamakawa, A., Yamashita, K., Makishima, A. & Nakamura, E. Chromium isotope systematics of achondrites: chronology and isotopic heterogeneity of the inner solar system bodies. *Astrophys. J.* **720**, 150–154 (2010).
51. Qin, L., Alexander, C. M. D., Carlson, R. W., Horan, M. F. & Yokoyama, T. Contributors to chromium isotope variation of meteorites. *Geochim. Cosmochim. Acta* **74**, 1122–1145 (2010).
52. Carlson, R. W., Boyet, M. & Horan, M. Chondrite barium, neodymium, and samarium isotopic heterogeneity and early earth differentiation. *Science* **316**, 1175–1178 (2007).
53. Boyet, M. & Carlson, R. W.  $^{142}\text{Nd}$  evidence for early (> 4.53 Ga) global differentiation of the silicate Earth. *Science* **309**, 576–581 (2005).
54. Borg, L. E., Brennecka, G. A. & Symes, S. J. Accretion timescale and impact history of Mars deduced from the isotopic systematics of martian meteorites. *Geochim. Cosmochim. Acta* **175**, 150–167 (2016).
55. Moynier, F. *et al.* Planetary-scale strontium isotopic heterogeneity and the age of volatile depletion of early Solar System materials. *Astrophys. J.* **758**, 45 (2012).
56. Paton, C., Schiller, M. & Bizzarro, M. Identification of an  $^{84}\text{Sr}$ -depleted carrier in primitive meteorites and implications for thermal processing in the solar protoplanetary disk. *Astrophys. J.* **763**, L40 (2013).
57. Hans, U., Kleine, T. & Bourdon, B. Rb–Sr chronology of volatile depletion in differentiated protoplanets: BABI, ADOR and ALL revisited. *Earth Planet. Sci. Lett.* **374**, 204–214 (2013).
58. Clayton, N. R. Oxygen isotopes in meteorites. *Annu. Rev. Earth Planet. Sci.* **21**, 115–149 (1993).
59. Fischer-Gödde, M., Burkhardt, C., Kruijer, T. S. & Kleine, T. Ru isotope heterogeneity in the solar protoplanetary disk. *Geochim. Cosmochim. Acta* **168**, 151–171 (2015).

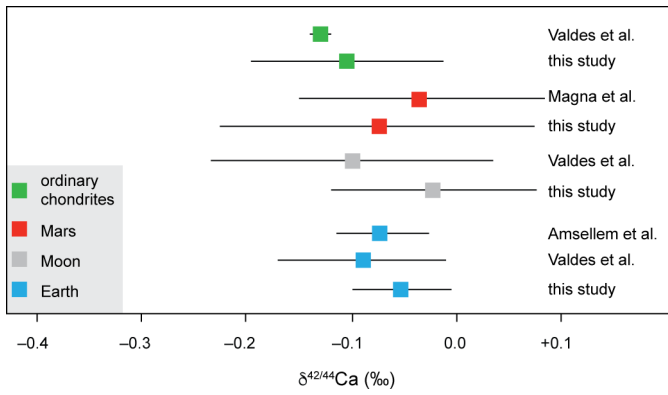


**Extended Data Figure 1 |  $\mu^{48}\text{Ca}$  values of planetary bodies versus mass for different masses of the ureilite parent body and Earth's precursor. a–c, Regressions (solid lines) and associated correlation coefficients through the data (squares) by assuming an ureilite parent body with a radius of 50 km and masses of  $M_{\text{Earth}}$ ,  $0.5M_{\text{Earth}}$  and  $0.25M_{\text{Earth}}$  for Earth's**

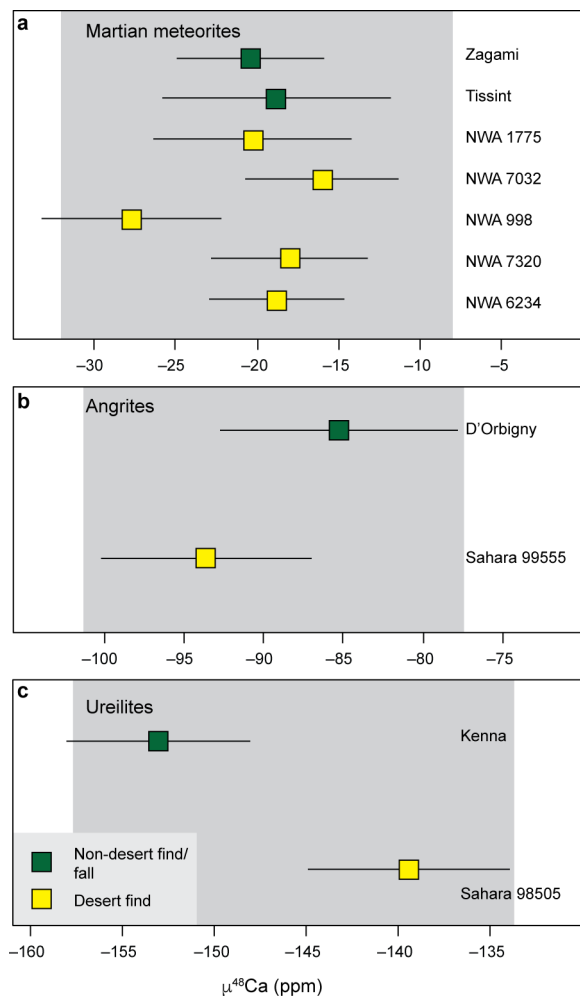
precursor. d–f, Regressions through the data but assuming a ureilite parent body with a radius of 105 km and masses of  $M_{\text{Earth}}$ ,  $0.5M_{\text{Earth}}$  and  $0.25M_{\text{Earth}}$  for Earth's precursor. The masses for the angrite parent body, Vesta and Mars are the same as in Fig. 2a.



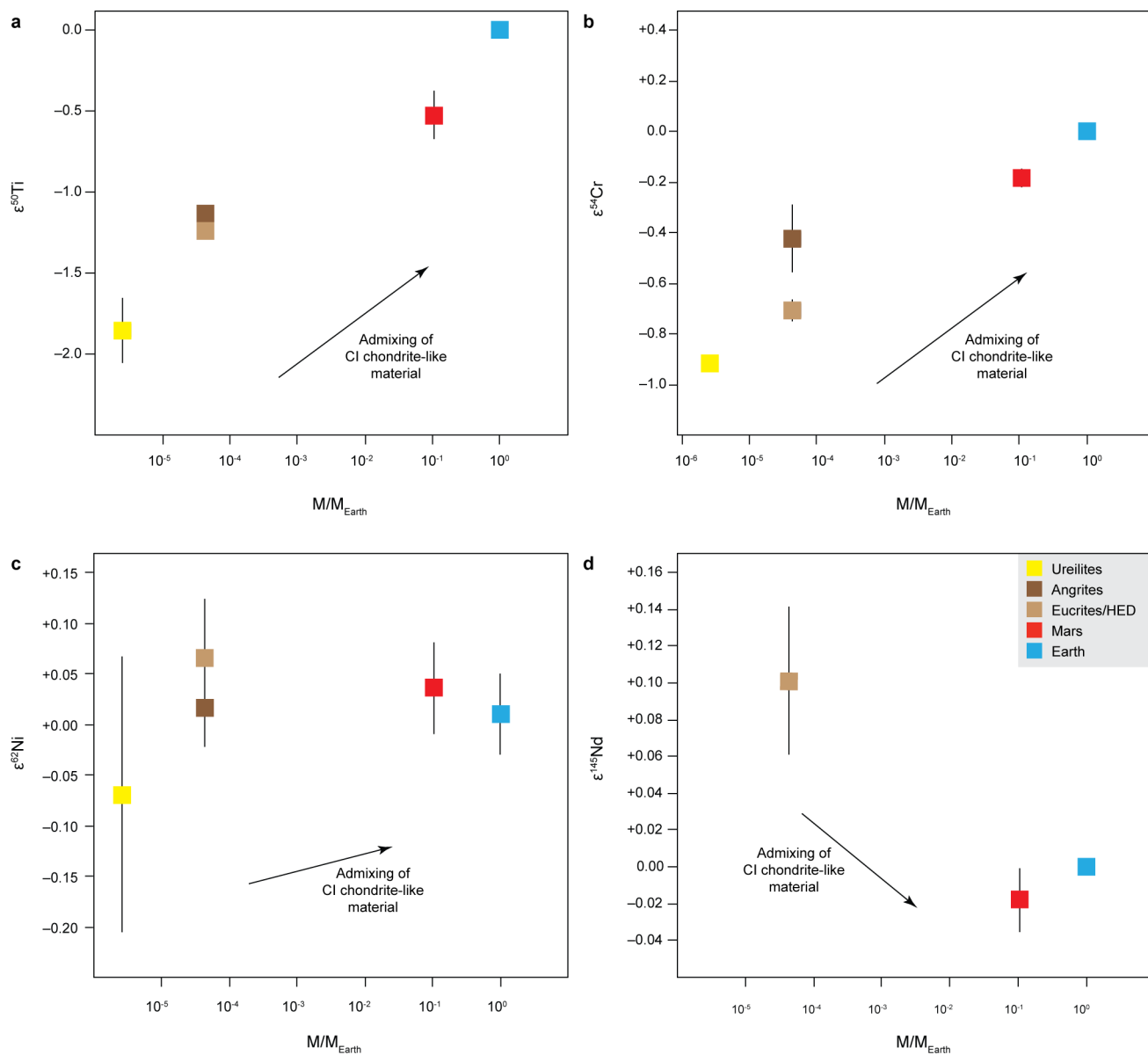
**Extended Data Figure 2 | Three-isotope plot of the average  $\delta^{42/44}\text{Ca}$  versus  $\delta^{43/44}\text{Ca}$  for Earth, meteorite parent bodies and chondrite groups relative to the standard SRM 915b.** The solid line shows the mass-dependent fractionation predicted by kinetic mass fractionation. Uncertainties shown for  $\delta^{42/44}\text{Ca}$  and  $\delta^{43/44}\text{Ca}$  are two times the standard error of the mean per group of analysed samples. For groups containing a single sample (ordinary chondrites, CI, CM and C2-ung), the error represents either the external reproducibility (0.05 and 0.03 for  $\delta^{42/44}\text{Ca}$  and  $\delta^{43/44}\text{Ca}$ , respectively) or the analytical uncertainty of the measurement; whichever is larger.



**Extended Data Figure 3 | Comparison of  $\delta^{42/44}\text{Ca}$  values with previous results.** Data for ordinary chondrites and martian, lunar and terrestrial basalts<sup>43-45</sup> are compared with those determined in this study. Uncertainties shown are two standard errors of the mean.



**Extended Data Figure 4 | Comparison of  $\mu^{48}\text{Ca}$  values determined for desert and non-desert finds or falls.** Data are shown for martian (a), angrite (b) and ureilite (c) meteorites. The grey shaded area indicates the external reproducibility of individual sample analyses. Uncertainties shown are two standard errors of the mean.



**Extended Data Figure 5 | Correlation between parent-body mass and nucleosynthetic anomalies for  $^{50}\text{Ti}$ ,  $^{54}\text{Cr}$ ,  $^{62}\text{Ni}$  and  $^{145}\text{Nd}$ .** The data are from refs 1, 2, 6, 46–54. The masses are shown relative to the mass of Earth,  $M_{\text{Earth}}$ . Arrows indicate the effects of mixing CI-like matter with

the inner-disk reservoir on the isotope composition, as predicted on the basis of measured nucleosynthetic signatures of CI chondrites. Error bars indicate the 95% confidence level of the mean.

Extended Data Table 1 | Mass-independent  $\mu^{48}\text{Ca}$  values and mass-dependent  $\delta^{42/44}\text{Ca}$  and  $\delta^{43/44}\text{Ca}$  data relative to SRM 915b

Sample	$\mu^{48}\text{Ca} \pm 2\text{SE}$	$\delta^{42/44}\text{Ca} \pm 2\text{SE}$	$\delta^{43/44}\text{Ca} \pm 2\text{SE}$
<b>Earth</b>			
BIR-1a (n=6)	+0.2 ± 1.7	-0.04 ± 0.02	-0.02 ± 0.01
BIR-1a†	+6.1 ± 5.7	-0.04 ± 0.02	-0.01 ± 0.02
BHVO-2†	+6.3 ± 7.5	-0.04 ± 0.04	-0.02 ± 0.02
BCR-2†	+5.2 ± 3.4	-0.08 ± 0.04	-0.04 ± 0.02
DNC-1†	+1.0 ± 4.0	-0.04 ± 0.03	-0.02 ± 0.01
BHVO-1†	-6.1 ± 8.1	-0.08 ± 0.03	-0.04 ± 0.02
SGR-1†	-4.6 ± 8.7	-0.02 ± 0.02	-0.01 ± 0.01
Sarm 40†	-6.7 ± 9.7	-0.08 ± 0.02	-0.04 ± 0.01
Mean	+0.2 ± 3.9	-0.05 ± 0.02	-0.03 ± 0.01
<b>Moon</b>			
NWA 4734 (n=7)	+3.4 ± 6.7	-0.08 ± 0.04	-0.04 ± 0.02
Dhofar 026 (n=2)	+6.4 ± 2.5	+0.03 ± 0.00	+0.02 ± 0.00
NWA 8632 (n=2)	+3.2 ± 3.3	+0.00 ± 0.13	+0.00 ± 0.06
Dhofar 287	+1.9 ± 4.7	-0.04 ± 0.03	-0.02 ± 0.02
Mean	+3.7 ± 1.9	-0.02 ± 0.05	-0.01 ± 0.02
<b>Mars</b>			
NWA 6234	-18.8 ± 4.2	-0.03 ± 0.01	-0.01 ± 0.00
NWA 7320	-18.0 ± 4.8	-0.03 ± 0.02	-0.02 ± 0.01
NWA 998	-27.7 ± 5.5	-0.01 ± 0.01	-0.01 ± 0.00
NWA 7032	-16.0 ± 4.7	-0.02 ± 0.01	-0.02 ± 0.01
NWA 1775	-20.3 ± 6.1	-0.08 ± 0.04	-0.04 ± 0.02
Tissint	-18.8 ± 7.0	-0.22 ± 0.04	-0.11 ± 0.02
Zagami	-20.4 ± 4.5	-0.12 ± 0.04	-0.06 ± 0.02
Mean	-20.0 ± 2.8	-0.07 ± 0.06	-0.04 ± 0.03
<b>Ordinary chondrites</b>			
Kramer Creek (L4) (n=4)	-34.5 ± 10.7	-0.14 ± 0.07	-0.07 ± 0.03
Bovedy (L3)*	-35.4 ± 2.9	-0.13 ± 0.01	-0.06 ± 0.01
NWA 4910 (LL3)	-44.3 ± 9.3	-0.04 ± 0.01	-0.02 ± 0.01
NWA 5697 (L3) (n=3)	-25.5 ± 8.2	-0.11 ± 0.03	-0.05 ± 0.01
Mean	-34.9 ± 7.7	-0.10 ± 0.05	-0.05 ± 0.02
<b>Eucrites</b>			
Juvinas*	-91.5 ± 7.1	-0.12 ± 0.03	-0.07 ± 0.02
Stannern*	-102.4 ± 4.3	-0.09 ± 0.02	-0.05 ± 0.01
Mean	-97.0 ± 10.9	-0.11 ± 0.03	-0.06 ± 0.02
<b>Angrites</b>			
D'Orbigny*	-85.3 ± 7.5	-0.07 ± 0.02	-0.04 ± 0.01
Sahara 99555*	-93.6 ± 6.6	-0.17 ± 0.08	-0.09 ± 0.04
Mean	-89.5 ± 8.3	-0.12 ± 0.10	-0.07 ± 0.05
<b>Ureilites</b>			
Kenna*	-153.0 ± 5.0	-0.21 ± 0.01	-0.11 ± 0.01
Sahara 98505*	-139.4 ± 5.5	-0.24 ± 0.03	-0.12 ± 0.02
Mean	-146.2 ± 13.6	-0.23 ± 0.03	-0.12 ± 0.01
<b>Carbonaceous chondrites</b>			
Ivuna (CI)*	+206.1 ± 8.5	+0.14 ± 0.04	+0.08 ± 0.02
EET 92161 (CR2)	+222.5 ± 4.0	+0.07 ± 0.02	+0.05 ± 0.01
NWA 1180 (CR2)	+206.6 ± 4.6	+0.13 ± 0.01	+0.07 ± 0.00
Tagish Lake (C2-ung)	+291.3 ± 5.3	+0.05 ± 0.01	+0.03 ± 0.01
Jbilet Winselwan (CM2)	+314 ± 14	+0.14 ± 0.01	+0.08 ± 0.00
<b>Chondrules</b>			
NWA 5697 (LL3)			
2-C1	-150 ± 59	-0.20 ± 0.01	-0.08 ± 0.02
5-C2	-145 ± 53	-0.31 ± 0.10	-0.11 ± 0.04
5-C10	-51 ± 70	-0.19 ± 0.04	-0.08 ± 0.02
D-C3	-154 ± 10	+0.02 ± 0.05	+0.01 ± 0.03
5-C4	-15 ± 31	-0.33 ± 0.04	-0.15 ± 0.02
3-C5	-151 ± 16	-0.12 ± 0.04	-0.01 ± 0.00
11-C1	+16 ± 33	-0.19 ± 0.03	-0.08 ± 0.02
11-C2	-119 ± 24	-0.13 ± 0.01	-0.05 ± 0.02
3-C2	-101 ± 19	-0.10 ± 0.01	-0.05 ± 0.01
NWA 6043 (CR2)			
1-C2	+227 ± 16	-0.10 ± 0.01	-0.04 ± 0.01
2-C4	+198 ± 24	-0.06 ± 0.01	-0.04 ± 0.01

$\mu^{48}\text{Ca}$  is expressed in parts per million, and  $\delta^{42/44}\text{Ca}$  and  $\delta^{43/44}\text{Ca}$  are in parts per thousand.  
SE, standard error.

\*Data from ref. 3.

†Data from ref. 34.